PHASES TRANSFORMATION OF NICKEL LATERITIC ORE DURING DEHYDRATION

Q. Huang and X. Lv[#]

*School of Materials Science and Engineering, Chongqing University, China, 400044

Abstract

The high magnesium nickel laterite ore need first be dehydrated if it is treated by the pirometallurgical means. The nickel laterite ore was dehydrated in a laboratory scale sintering pot in this study. The dehydration mechanism was studied by using the thermo-gravimetric (TG) tests, differential thermal analysis (DTA), and X-ray diffraction (XRD) experiments. The measurements indicated that chlorite $(Fe,Mg,Al)_6(Si,Al)_4O_{10}(OH)_8$ and serpentine $Mg_{21}Si_{12}O_{28}(OH)_{34}H_2O$ are the primary phases, while $FeO(OH)$ and $(Fe,Mg,)_3Si_4O_{10}(OH)_2$ are the minor phases in the ore. The water in the ore can be divided as free water, crystal water, and hydroxyl group. During the heating process, the temperature range for the removal of the free water is 25~140 °C, for the crystal water it is 200~480 °C, and for the hydroxyl group it is 500~800°C. The experiments with various coal dosages show that the temperatures of off-gas and burden increase with an increase in coal dosage. The sinter samples were analyzed using XRD. The results demonstrated that olivine $(Mg,Fe)_2SiO_4$ and spinel $MgFe_2O_4$ are the main bonding phases.

Key words: Nickel laterite, Ferronickel making, Dehydrating, Sintering

1. Introduction

Nickel lateritic ore are formed during lateritic weathering of ultramafic and mafic igneous rocks (peridotites, serpentinites, pyroxenites, and gabbros). Today, 40 % of the world Ni-production originates from, and 54 % of the total reserves are found in laterites [1]. Sulfide deposits and oxide ores are the two main resource of nickel.

[#] *Corresponding author: lvxuewei@163.com*

Approximately 36% of the world's nickel laterite reserves occur as sulphide, and 64% occur as oxide ores [2]. Demand for nickel had risen from under 200,000 tons/year in 1950 to over 1,200,000 tons/year in 2003 [3, 4]; it will reach 1,454,000 tons in 2008. The worldwide output of the stainless steel was over 277,000,000 tons in 2007, and will reach 287,000,000 tons [5]. The enormous gap between demand and supply drives the price of the nickel higher in the world market. Therefore, the dominance of sulfide ores as the major source of nickel was not challenged until several years ago. Because 70% of the world's land-based nickel resources are contained in laterites, they currently account for only about 40% of world nickel production [4, 6]. Laterite ores cannot be concentrated like sulphide; rather, they must be processed as mined. Therefore, it's vitally important to develop a practical and inexpensive process for using laterite.

Most plants produce nickel or ferronickel by pyrometallurgical means using a rotary kiln and electric furnace. Extraction of nickel or ferronickel from the high-magnesia lateritic nickel ores by this means requires a great deal of energy. For example, the original moisture content of ores is 30%; it is demanded to dry to a moisture content of 20%, using 3.71MJ per kilogram of water removed [2]. Sintering is an important procedure used by the iron-making industry to agglomerate fine ores. This process removes water from the mixture of the iron ores, fluxing agent, and the coals at the same time [7, 8]. Energy requirements may decrease if the nickel laterite ores are hydrated and sintered by means of traditional sintering, and if the nickel lateritic sinters are then reduced in the shaft furnace. To facilitate this process, the present work examines the dehydrating and sintering mechanism of nickel laterite.

2. Experimental

Since combustion heat is absorbed when nickel laterite ores are mixed with coal in certain proportions, the mixture was heated and sintered from top to bottom by the method of air exhaust. Thus, the water, which may have existed as free water, crystal water, or hydroxyl group, was removed from the mixture, and the burden was agglomerated as sinter with some mechanical strength and permeability. The mineral composition of the nickel laterite samples before sintering was determined with chemical analysis, thermo-gravimetric (TG) tests, differential thermal analysis (DTA), and X-ray diffraction (XRD). After sintering, the samples were examined by XRD.

The TG and DTA were carried out using NETZSCH STA 449C with heating speed of 25K/10min and a maximum temperature of 900˚C. The XRD analysis was carried out using D/MAX 3C (Co Ka). The sintering experiments were performed in a laboratory scale sintering pot shown in Fig.1.

The sintering experiments were conducted separately with coal dosages of 8%, 11%, 14%, and 17% respectively. The experiments proceeded as follows:

(1) Materials mixing: Nickel laterite and coal were weighed and mixed homogenously.

(2) Mixture loading: First, a 6-10mm deep layer of sinter was charged over the fire grate. The mixture was then loaded until the sintering pot was full. Finally, coal was laid

on top of the mixture to a depth of 5 mm. The total height of the burden was 380 mm, with 0.3 kg igniting coal. Segregation of the mixture and compacting of burden were carefully avoided.

(3) Igniting: The sintering pot was installed on the base frame of the apparatus. The exhaust fan was turned on and the manometer was adjusted to reach 800 mm H_2O, or about 7839.5 Pa. Ignition temperature was 1100-1200 ˚C, and ignition continued for 1 minute. Following ignition, the data acquisition system was turned on to record the temperatures measured by the thermal couples A-D.

(4) Sintering: The mixture was sintered from top to bottom with continuous exhausting. The temperature was recorded every 500 ms. Sintering ended when the temperature of the off-gas decreased dramatically and never rose. The exhaust fan was then turned off, and the sinter was allowed to cool naturally to room temperature.

(5) Measuring: The sinters were screen separated and weighed. Samples were selected for measurement.

3. Results and discussion
3.1 Analysis of raw materials

The chemical analysis of the nickel laterite and coal used here is shown in Tables 1 and 2. The results of XRD and TG-DTA are
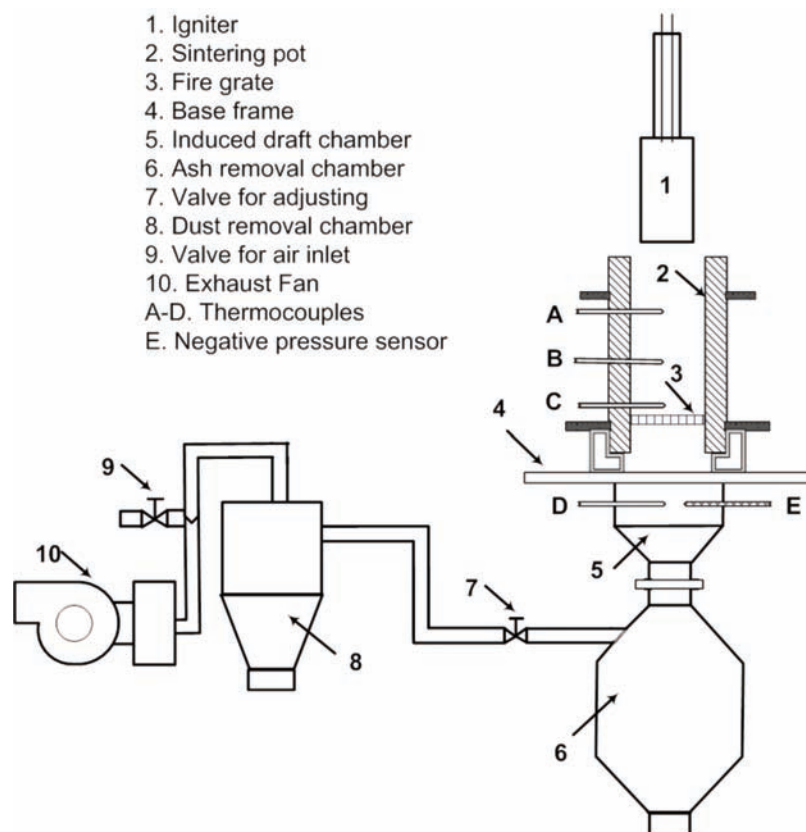

1. Igniter
2. Sintering pot
3. Fire grate
4. Base frame
5. Induced draft chamber
6. Ash removal chamber
7. Valve for adjusting
8. Dust removal chamber
9. Valve for air inlet
10. Exhaust Fan
A-D. Thermocouples
E. Negative pressure sensor

Figure 1. Schematic of laboratory scale sintering pot

Table 1 Chemical composition of the nickel laterite, %

Cr_2O_3	SiO_2	P	TFe	Al_2O_3	CaO	MgO	Ni	Crystal water
1.93	30.35	0.01	20.78	1.8	0.95	19	1.31	8.76

Table 2 Chemical composition of coal, %

C	S	Ash	Volatile	Water
76.19	0.51	14.36	9.52	0.83

shown in Figs.1 and 2.

The XRD pattern reveals that this nickel laterite is a typical saprolitic ore, containing dominant amounts of Mg silicate and Mg-Fe silicate minerals [9]. In saprolitic ores, Ni occurs mainly in Mg silicates, and Cr occurs mainly in Fe silicates or goethite. The mineral species contains much crystal water and hydroxyl group. In addition, some aluminates are present. Therefore, this "wet" nickel laterite is a kind of ultra-basic rocks [10, 11]. In tropical and subtropical areas, this mineral will typically be found between the groundwater level and the surface of the earth.

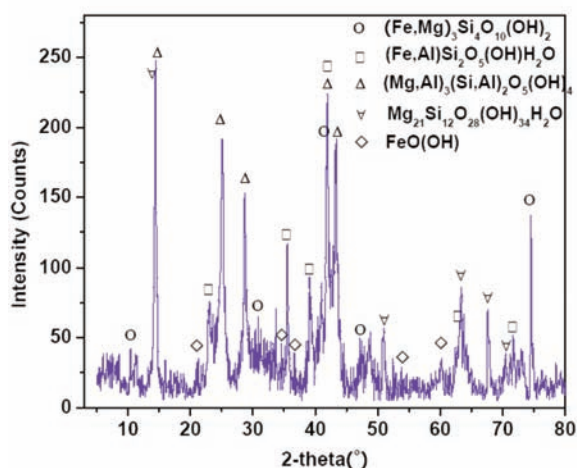As shown in Fig.3, there are three obvious endothermic reactions and one exothermic

Figure 2. XRD pattern for the nickel literate

reaction in the DSC curve. The first reaction occurs at 86.3 ˚C, with 8.9% mass loss in the TG curve; this is the evaporation of the free water. The second reaction occurs at 256.4 ˚C, with 4.29% mass loss due to the crystal water. The third occurs at 602.1 ˚C, with 4.10% mass loss, caused by the loss of hydroxyl group. In addition, there is another small endothermic reaction at around 310 ˚C due to a small amount of goethite FeO(OH), which loses the crystal water at 309 ˚C. The nickel laterite is composed of several minerals with crystal water that will be lost at various temperatures, most between 200 ˚C and 480˚C. The exothermic reaction occurs at 821.0 ˚C due to the decomposition of silicate, and involves no mass loss; however, there is a 0.48% mass loss with the reaction at the TG curve. The likely reason for this phenomenon is the removal of hydroxyl remaining in the minerals. Therefore, the total mass loss for the hydroxyl group is 4.10%+0.48%=4.58%.

A comparison of the measurements with the atlas of TG-DTA for minerals [12] prompted several conclusions: The removal of hydroxyl group of chlorite $(Fe,Mg,Al)_3(Si,Al)_2O_5(OH)_4$ began from 602 ˚C and finished at 760 ˚C. The chlorite group then decomposed into MgO and SiO_2 at 821 ˚C. All the crystal water of serpentine $Mg_{21}Si_2O_{28}(OH)_{34}H_2O$ were lost above 480 ˚C, forming $Mg_3Si_2O_5(OH)_4$, and the hydroxyl was removed between 600 ˚C and 700 ˚C. With this reaction, $Mg_3Si_2O_7$ formed, then decomposed at 795 ˚C. The
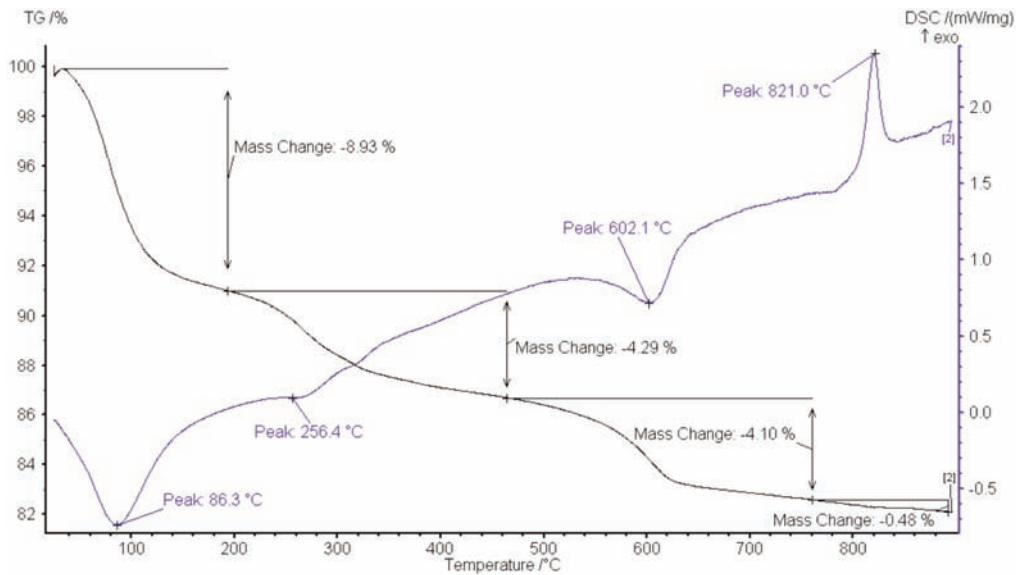
Figure 3. TG-DTA pattern for the nickel laterite

gramenite $(Fe,Al)Si_2O_5(OH)H_2O$ lost crystal water at 143 ˚C, and it lost the hydroxyl at 480-510 ˚C. Goethite lost crystal water at 309˚C. A combination of XRD patterns and the TG-DTA indicated that chlorite $(Fe,Mg,Al)_3(Si,Al)_2O_5(OH)_4$ and serpentine $Mg_{21}Si_2O_{28}(OH)_{34}H_2O$ are the main mineral phases and that $FeO(OH)$ and $(Fe,Mg,)_3Si_4O_{10}(OH)_2$ are the minor phases in nickel laterite.

The mass of crystal water and hydroxyl is 4.29%+4.10%+0.48%=8.87%, slightly more than the 8.76% measured by chemical analysis, and the error is 0.12%. Over 90% of the water is removed when the temperature rises above 650 ˚C.

3.2 Temperature of the burden and off-gas

During the sintering experiments, the temperatures of the off-gas and the burden were measured by the thermal couples A, B, C, and D, as shown in Fig.1. The relationship

between the temperature of off-gas (measured by thermal couple C) and the coal dosage in the mixture is plotted in Fig.4. The temperature of the off-gas began to increase quickly 25 minutes after ignition. The maximum temperature of the off-gas increased as the coal dosage increased, and the time required to reach the maximum temperature was reduced. For example, with
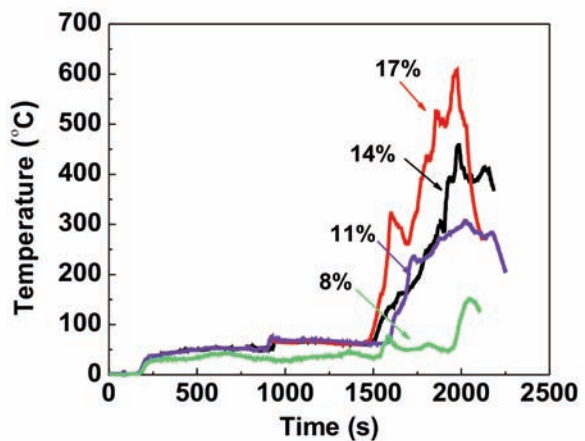

Fig.4. Relationship between off-gas temperature and coal dosage

a coal dosage of 17%, the off-gas reached the maximum temperature of 604 ˚C at 32.3 minutes. With a 14% coal dosage, however, it reached the maximum temperature of 450 ˚C at 33.6 minutes. With a coal dosage of 11%, the off-gas reached the maximum temperature of 302 ˚C at 33.58 minutes, and with an 8% coal dosage, the maximum temperature was only 145 ˚C, which it reached in 34.17 minutes.

As shown in Fig.5, the change in the temperature of burden in the sintering pot was complex because many exothermic or endothermic reactions occur during the sintering. In the case of a 14% coal dosage, the temperature of the burden reached its first peak of 1050 ˚C at 8 minutes, then decreased quickly to 377 ˚C just 2.5 minutes later. It reached the second peak of 1035 ˚C after another 8 minutes. With an 11% coal dosage, the burden reached the first peak of 950 ˚C 18 minutes after ignition, then decreased quickly to 733 ˚C, reaching its second peak of 1173 ˚C only 2 minutes later. It reached the third peak of 736 ˚C at 25.6

Figure 5. Relationship between burden temperature and coal dosage

minutes. With a coal dosage of 8%, the burden reached the first peak of 783 ˚C at 25.5 minutes, the second peak of 751 ˚C 4.5 minutes later, and the third peak of 800 ˚C after 32.88 minutes. In the case of a 17% coal dosage, the outside of sintering pot was heated red, and the thermal couple was damaged by the high temperature. The temperature of burden, therefore, was likely over 1200 ˚C, and probably between 1400 ˚C and 1600 ˚C. The fluctuation in temperature was caused by the dehydration. High temperatures favor the dehydration, which in turn cools the burden. The movement of the free water also has a significant effect on the temperature changes. The free water of the top burden absorbs the heat, turns into steam, and finally removes the heat. The steam condenses when it reaches the cool burden at the bottom, releasing the heat to the burden. As a result, the amount of water contained in the burden continues to increase. Once the temperature is high enough, the water vaporizes again, but the temperature drops quickly. A high coal dosage reduces the frequency of this fluctuation, favoring the sintering process.
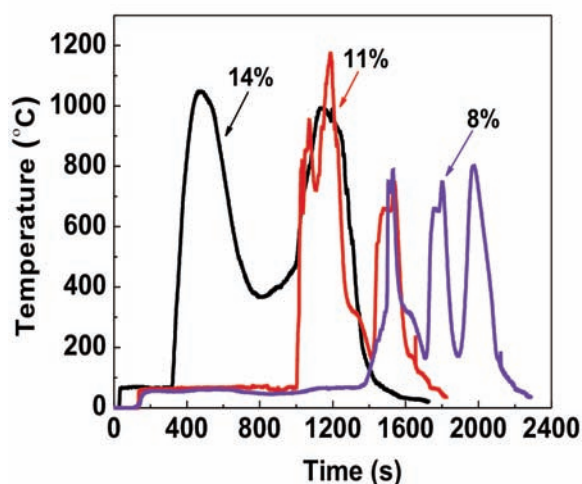
3.4 Sinter phase analysis

After natural cooling to room temperature, the products of sintering with coal dosages of 17% and 8% were sampled for XRD and SEM-EDS. As shown in Fig.6, XRD patterns clearly shows that hydroxyl remained in the $(Fe,Mg)_3Si_4O_{10}(OH)_2$, although it should have lost at over 1000 ˚C. The hydroxyl may have been retained because the minerals were bonded quickly by the liquid phases created, worsening the

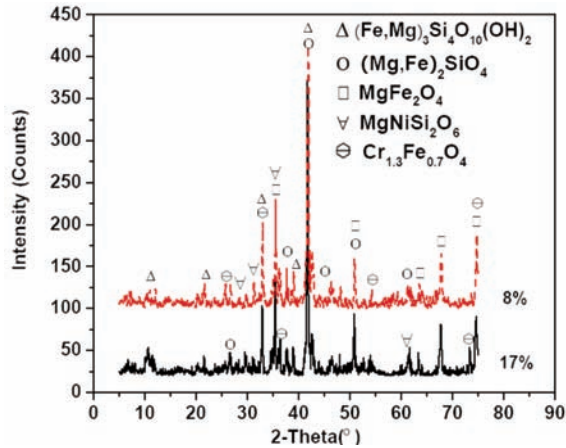kinetic condition of the dehydration. The main phases in the sinter are $(Fe,Mg)_2SiO_4$ and $MgFe_2O_4$.

Figure 6. XRD patterns for sinters

4. Conclusions

This work studied the phases transformation of nickel laterite ore during the dehydrating process in the sintering pot, the conclusions are summarized as follows:

1. Chlorite $(Fe,Mg,Al)_3(Si,Al)_2O_5(OH)_4$ and serpentine $Mg_{21}Si_2O_{28}(OH)_{34}H_2O$ are the primary phases, and $FeO(OH)$ and $(Fe,Mg,)_3Si_4O_{10}(OH)_2$ are the minor phases in nickel laterite.

2. When the nickel laterite is heated at 25 ˚C /10min, the removal efficiency of water will reach 90% when the temperature exceeds 650 ˚C and 99% when it exceeds 900 ˚C.

3.The temperatures of the off-gas and sintering mixture increase as the coal dosage increases.

4. Olivine $(Mg,Fe)_2SiO_4$ and spinel $MgFe_2O_4$ are the main bonding phases in the nickel laterite sinter.

Reference

[1] I. Ilic, K. Cerovic and S. Stopic., J. Min. Metall. Sect. B., 39 (3-4) (2003) 427.

[2] R.A. Bergman: Canadian Mining and Metallurgical Bulletin, 96(2003) 127.

[3] R.G. Mcdonald and B. I. Whittington: Hydrometallurgy, 91(2008), 56.

[4] R.G. Mcdonald and B. I. Whittington: Hydrometallurgy, 91(2008), 35.

[5] W.Z. Zhao: World Nonferrous Metals, (2007) 6.

[6] A.D. Dalvi, W. G. Bacon and R. C. Osborne: International laterite nickel symposium, TMS, (2004) 23.

[7] X. Lv, C. Bai, G. Qiu et. al.: ISIJ International, 49(2009) 703.

[8] G. B. Qiu, Y. Xu., J. Min. Metall. Sect. B., 46 (1) (2009) 131.

[9] T.T. Chen, J. E. Dutrizac and E. Krause: International laterite nickel symposium, TMS, (2004) 79.

[10] F. Habashi, J. Min. Metall. Sect. B-Metall. 45 (1) B (2009) 1.

[11] Z.Horvath, B. Varga and A. Mindszenty: Chemical Geology, 170 (2000) 81.

[12] G. Chen and Y. Zhang: Atlas of minerals thermal analysis and phase change, 1st ed., eds., Press of science and technology, Chengdu, China (1989) 459.